Ain Shams Engineering Journal 16 (2025) 103314

Contents lists available at ScienceDirect

Ain Shams Engineering Journal

journal homepage: www.sciencedirect.com

Full Length Article

Current transformer saturation detection by cross-correlation with independent target signal

Mahmoud M. Elgamasy [a], Mohamed S. Zaky [b,*], Ahmed F. Zobaa [c], Mahmoud A. Elsadd [d]

[a] Electrical Engineering Department, Faculty of Engineering, Menoufia University, Egypt
[b] Electrical Engineering Department, College of Engineering, Northern Border University, Arar 1321, Saudi Arabia
[c] Electronic and Electrical Engineering Department, Brunel University of London, Uxbridge, United Kingdom
[d] Electrical Engineering department, Faculty of Engineering, Damanhour University, Egypt

ARTICLE INFO

Keywords:
Current Transformer
Saturation Detection
Cross-correlation
Kalman Filter

ABSTRACT

The saturation of current transformers (CTs) leads to distortion in secondary current, potentially causing malfunction in protective relays within power systems. Detecting the saturated portions in the measured signal and reconstructing the primary reference current are essential to prevent relay malfunctions and ensure sensitivity during faults. Existing methods in the literature still face challenges in improving accuracy, especially in the presence of noise in the measured signal. The proposed method in this paper is more robust under noisy conditions compared to existing signal processing-based methods. It relies on a cross-correlation algorithm that uses an independent target signal. This method is parameter-less and independent of the CT's specifications. Additionally, no extra hardware equipment is required. The proposed method identifies the saturated portions in the measured secondary current in each cycle, enabling the reconstruction of the saturated current to obtain the reference primary current. A test system has been simulated, and the data are processed using MATLAB. Various test cases are executed, and the results confirm that the proposed method is highly effective in providing fast and accurate detection of CT saturation, with improved robustness against noise.

1. Introduction

Current transformers (CTs) are indispensable components, serving a vital role in measuring and monitoring current flow in electrical power systems and various other control applications [1–3]. Their ability to deliver reliable current information is essential for ensuring the reliability of the protection of electrical power systems. CT saturation is a phenomenon that occurs when the core material of the CT becomes magnetically saturated due to excessive current flow. When saturation occurs, the CT's ability to accurately transform current is reduced, causing distortion in the output signal. This distortion can result in inaccurate measurements and create a risk to the protection of the power system, potentially leading to the malfunction of protective relays [4–6]. Identifying the saturated portions in the CT secondary current signal and extracting the primary reference current are essential for preventing maloperation of protective relays and ensuring sensitivity during faults. Additionally, reconstructing the saturated current to align with the primary reference current is vital for maintaining accuracy and reliability in power system protection.

By addressing saturation issues, power system operators can maintain the integrity of current measurements and enhance the overall performance of protection systems. To mitigate saturation effects, engineers employ various techniques such as selecting CTs with appropriate ratings, ensuring proper CT sizing for the application, or employing current transformers with air gapped-core design [7,8]. However, the addition of the air gap using precise technology, as described in [7,8], increases manufacturing costs and magnetic leakage losses, and may also require a larger CT size to match the performance of conventional CTs. The widely employed methods to address the saturation and correct the induced errors, in iron-core CT, depend on implementing compensation circuits or digital signal processing algorithms. The methods presented in [9–11] are examples for hardware solutions. Hardware compensation circuit is utilized to avoid the occurrence of CT saturation. It is featured by its applicability with different relays technologies; however, the need for extra component and hardware circuit increases complexity and cost. On the other hand, signal processing-based methods have been introduced in [12–15]. In [12], morphological techniques are applied to highlight significant

* Corresponding author.
E-mail address: mohamed.zaky@nbu.edu.sa (M.S. Zaky).

https://doi.org/10.1016/j.asej.2025.103314
Received 19 April 2024; Received in revised form 4 January 2025; Accepted 6 February 2025
Available online 24 February 2025

changes in secondary current and detect the saturation. Likewise, the derivative-based and wavelet transform methods are sensitive to distortion and noise in measured signals [13–15]. However, noise can cause false detections of edges, leading to incorrect decisions [16,17].

Artificial intelligence and Data training-based methods are presented for detecting the CT saturation and reconstructing the secondary current as in [18–23]. An adaptive network-based fuzzy inference system is trained to reconstruct distorted current waveforms caused by CT saturation in [18]. In [19], a reverse extraction method combining Random Forest Classification (RFC) and PSO-LSTM is utilized to address CT saturation. It requires offline training with diverse CT operating conditions and online wavelet-based segmentation to reconstruct the primary current. In [20], a deep learning-based approach using stacked denoising autoencoders and Bayesian optimization is trained for detecting saturation. A Gaussian Mixture Model (GMM)-based approach is adopted in [21] for detecting CT saturation and it is trained on secondary current data through simulations under various fault conditions. In [22], a neural network is genetically optimized to create a saturation detector of CT. In [23], a data-driven model is created based on utilizing fully convolutional network to detect the saturation in current transformer. Database is required for training and Levenberg-Marquardt nonlinear least squares algorithm is employed to reconstruct the current. However, this method in [23] is limited by its time delay due to the included high computational burden. Furthermore, these methods presented in [18–23] require large datasets for training and may need additional data if CT parameters change. In general, AI and big data methods face inherent limitations across various applications [24,25]. Table 1 summarizes the limitations of existing studies compared to the proposed method in this paper. Thus, introducing a signal processing-based CT saturation detection approach that is independent of CT parameters and offers robust performance under noise poses a significant challenge for protection engineers.

The main contribution of this paper is providing a fast correlation-based approach to detect the saturation in current transformers with enhanced robustness against noise. The measured secondary current is processed and the saturated portions in the signal are effectively identified. The proposed method is distinguished by depending on a general target signal without the need to the parameters of the current transformer. Effectively determining the saturated portions in the measured signal supports reconstructing the saturated current to obtain the reference primary current. Hence, the reliability of power system protection is improved without the need for additional hardware equipment.

Table 1
Summarized comparison between the existing studies and the proposed method.

Existing studies	Limitations of the existing studies	The superiority of the proposed method over existing methods in the literature
[7,8] Air-gapped iron core CT methods	A specialized design with modifications to the CT's iron core is necessary.	The proposed signal processing method can be easily implemented with the existing iron-cored CTs in use.
[9–11] Additional hardware-integrated circuit-based methods	An additional hardware circuit integrated with the CT is required.	No additional hardware circuits are required.
[6,12–15] Signal processing methods based on derivative and wavelet analysis	They are highly susceptible to noise, even at low levels.	The proposed method demonstrates more robust performance under low levels of noise.
[18–23] Data-driven methods	These methods require large datasets for training and may need additional data if CT parameters change.	No training data is required, and it is independent of CT parameters.

The paper is organized as follows: Section 2 explains the cross-correlation concept. Section 3 presents the proposed CT saturation detection method. Section 4 describes the test system utilized and the CT under saturation. Section 5 details the independent target signal used for correlation. Section 6 provides the validation results for saturation detection. Section 7 explains how the saturated portions are identified. Section 8 demonstrates how the saturated secondary current is reconstructed to match the reference primary current. Section 9 offers a comparative analysis with related algorithms in the literature, and Section 10 concludes the paper.

2. Cross-Correlation

Correlation is one of the major algorithms used in discrete signals processing for various applications [26,27]. It is utilized to detect a signal, which is called the target signal, within another signal. Fig. 1 indicates the basic concept of the correlation algorithm. x is the input signal, y is the output signal, and t is the target signal that we looking to detect within the input signal. The output signal, y, is called the cross-correlated signal. The proposed saturation algorithm is based on the response of the cross-correlated signal. If the input signal contains the feature of the target signal, the cross-correlated signal is maximized at the corresponding moment.

The concept of correlation is elaborated in Fig. 1. The window containing the target signal samples is shown at the middle of the figure. The cross-correlation is performed by multiplying the samples of the input signal with the corresponding target samples and then adding the obtained values along the window size. To obtain the output, the target signal window is shifted to the next time step which is determined by the utilized sampling frequency level. The cross-correlated signal is calculated as:

$$y[j] = \sum_{k=o}^{k=n-1} x[j+k]t[k] \tag{1}$$

where y is the cross-correlated signal, x is the input signal, t is the target signal, j is the time index of the most recent sample, k is the sample index of the target signal changing from 0 to $n-1$, and n is the window size of the target signal. Eq. (1) represents the simple correlation method.

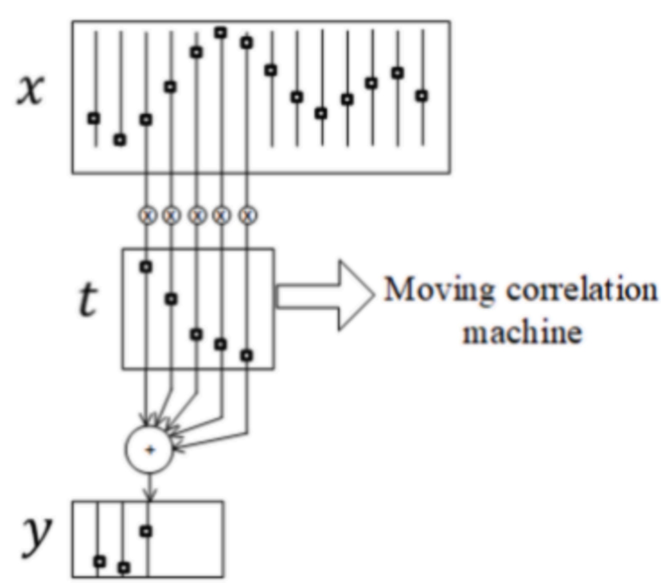

Fig. 1. Concept of utilized correlation machine.

3. Proposed CT saturation detection method

The detailed steps of the proposed detection method of CT saturation are illustrated in Fig. 2. The calculations and processing are performed every time step. A specific data window, with size of n samples, is needed for the measured secondary current samples. The window of the measured current is updated, every time step, by shifting the old samples and assigning the new measured sample in the most recent order as:

$$\begin{aligned} i_2[i] &= i_2[i+1]_{0\le i\le(n-1)} \\ i_2[n] &= newsample \end{aligned} \tag{2}$$

where i_2 is the measured CT secondary current, i is the sample index, and n is the index of the most recent sample in the window. For more clarification, this step is clarified in Fig. 3.

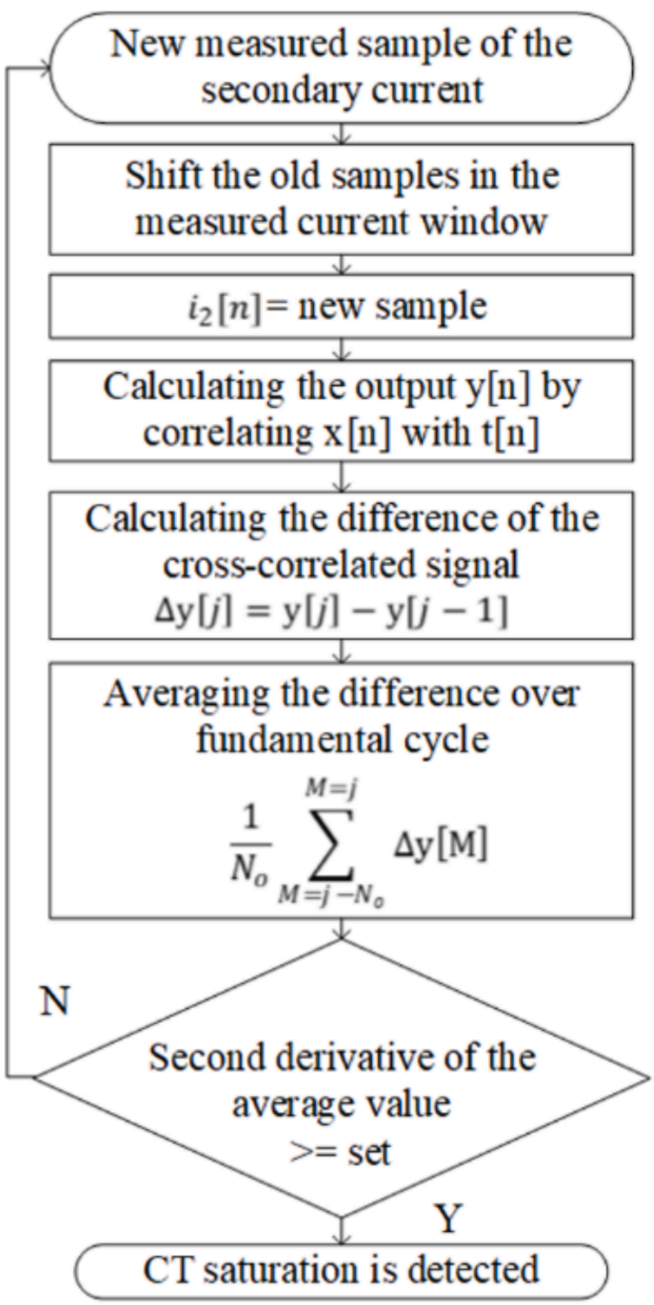

Fig. 2. Proposed CT saturation detection method.

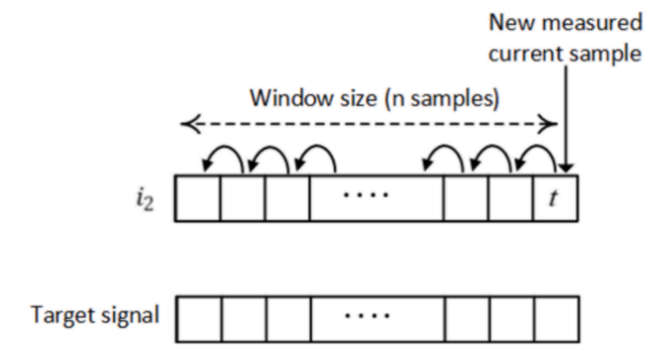

Fig. 3. Updating the window of measured CT secondary current to be correlated with the corresponding target signal.

Then, the measured current window is cross correlated with the target signal according to the adopted correlation scheme. The proposed detection scheme is dependent on the change of the obtained cross-correlated signal where the difference is calculated as:

$$\Delta y[j] = y[j] - y[j-1] \tag{3}$$

After that, the potential sinusoids components in the obtained cross correlated signal is eliminated by taking the average. This step is important as it supports noise suppression in the obtained signal. The difference signal is averaged over a fundamental cycle by:

$$average[j] = \frac{1}{N_o}\sum_{M=j-N_o}^{M=j}\Delta \mathrm{y}[\mathrm{M}] \tag{4}$$

where N_o is the number of samples per a fundamental cycle duration and j is the most recent time instant. The proposed method stands apart from existing signal processing-based approaches due to its superior performance with the presence of noise. By averaging the resulting difference of the correlated signal, the noise is effectively suppressed, leading to a more robust detection method in noisy conditions. Finally, the instants that indicate the saturated portions of the signal are clearly identified through the second derivative of the averaged signal. When the second derivative exceeds a preset threshold, saturation is confirmed.

4. CT under saturation

A 15 VA current transformer with a 2000/5A ratio is simulated using MATLAB. The burden at the secondary terminals of the CT is represented by a 1 Ω resistance. The primary current of the current transformer is obtained by simulating a fault current through a 120 kV, 50 Hz RL circuit with a reactance of 69.3 Ω and a resistance of 6.93 Ω. The simulated circuit is shown in Fig. 4a, based on the following assumptions: the current transformer under saturation is simulated using the saturable transformer tool in MATLAB, employing a single-core saturable transformer model. The model incorporates winding resistance and leakage inductance, with values of 0.001 pu and 0.04 pu, respectively. The saturation characteristic of the saturable transformer block is defined by a piecewise linear relationship between the flux and magnetization current, as depicted in Fig. 4b.

A test case is simulated by closing the switch. To obtain the current with maximum DC component, the instant of closing the switch is selected to be at the voltage zero-crossing point. The switch is closed at 0.02 s and the CT flux and currents are observed as shown in Fig. 5a and b, respectively. As shown in Fig. 5a, the CT flux rises until reaching the saturation level which is 10 pu. Consequently, the secondary current i_2 deviates from the reference signal i_r at 0.09108 s as depicted in Fig. 5.

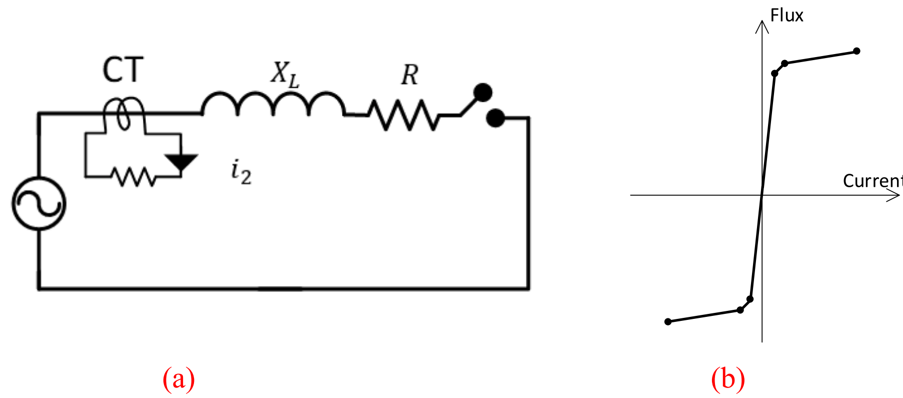

Fig. 4. The simulated test system for CT saturation; (a) the simulated circuit for the primary side of the CT; (b) the saturation characteristic of the modelled CT.

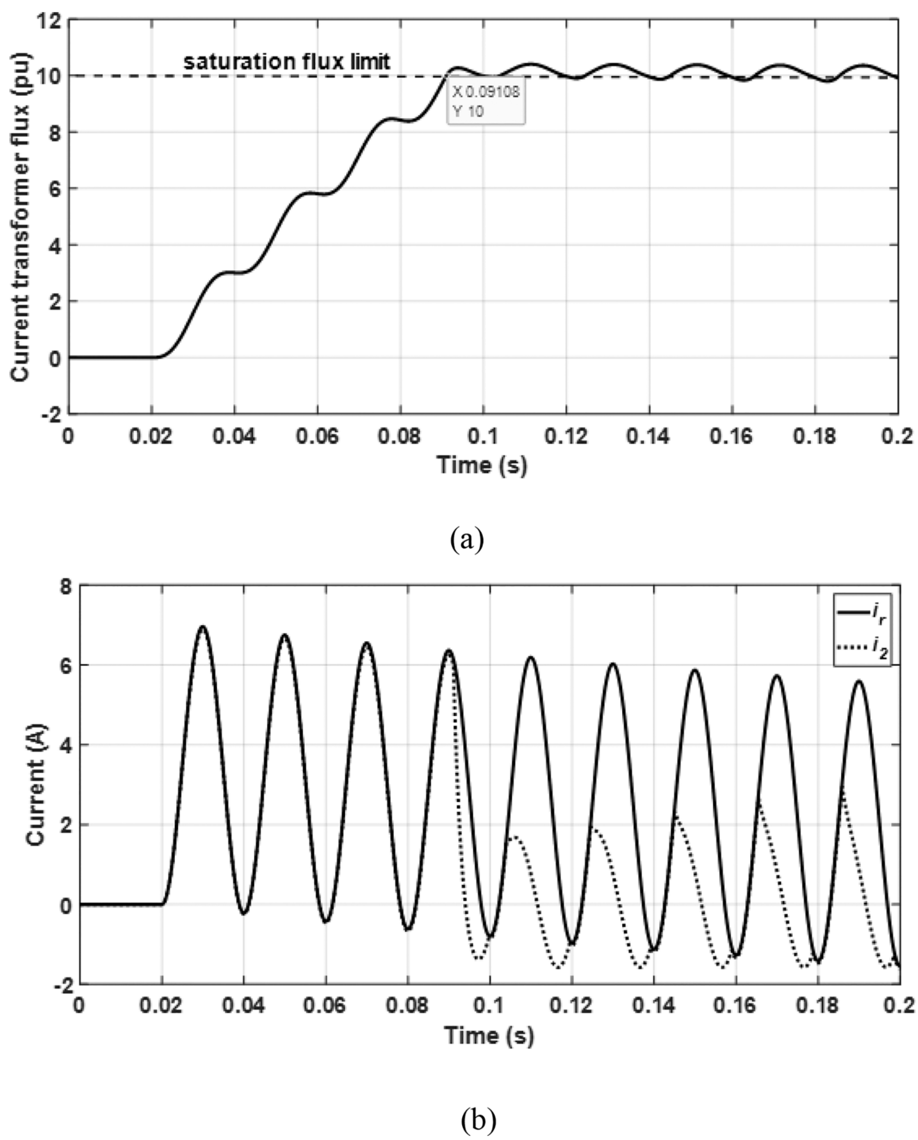

Fig. 5. (a) The CT magnetic flux after fault occurrence; (b) secondary current and reference current under CT saturation condition.

5. Proposed independent target signal

The proposed detection scheme is featured by its universality because the proposed target signal is independent of the CT characteristics. The target signal should include the features of the saturated current signal. The saturated portion of the current signal looks like a complementary exponential signal. The proposed target signal is formulated as follows:

$$Targetsignal = 1 - e^{\frac{t}{\tau}} \tag{5}$$

The time constant, τ, of the exponential function is selected to be 1 ms. As shown, the target signal is independent of the CT parameters, which is a significant advantage of the proposed saturation detection scheme.

6. Validation results

The proposed correlation algorithm is implemented on the previously obtained results in Fig. 5b. The measured CT secondary current is processed according to the proposed method with the proposed target signal in (5). The performed signal processing is conducted by MATLAB. The utilized sampling frequency under this test condition is100 kHz which corresponds to a time step of 10 μs.

The results are presented in Fig. 6, where Fig. 6a displays the output of the cross-correlation after correlating the measured CT secondary current with the target signal. To monitor the variation in the cross-correlated signal, the difference is computed using Eq. (3). As illustrated in Fig. 6b, the difference signal exhibits a sinusoidal waveform when the CT is not saturated. However, around 0.091 s, which corresponds to the point of saturation onset, the signal shows a significant deviation. According to the adopted method, the difference signal is averaged over a full cycle to remove sinusoidal variations and any potential noise. The resulting average of the difference signal for this test case is show in Fig. 6c. As observed, it maintains a negligible DC value before saturation occurs but starts to show significant changes after saturation onset. Lastly, the second derivative of the averaged signal is computed and compared to the threshold level, as shown in Fig. 6d. Based on the investigations, the threshold is set at 2×10^6, as indicated by the dotted line in the figure. By comparing the second derivative of the signal with this threshold, the output detector is generated. Fig. 6e illustrates both the CT secondary current and the output detector from the proposed method. As shown, the moments when saturation begins and ends in each cycle are accurately identified. This is a great advantage of the proposed method where the portions of CT saturation can be identified in each cycle.

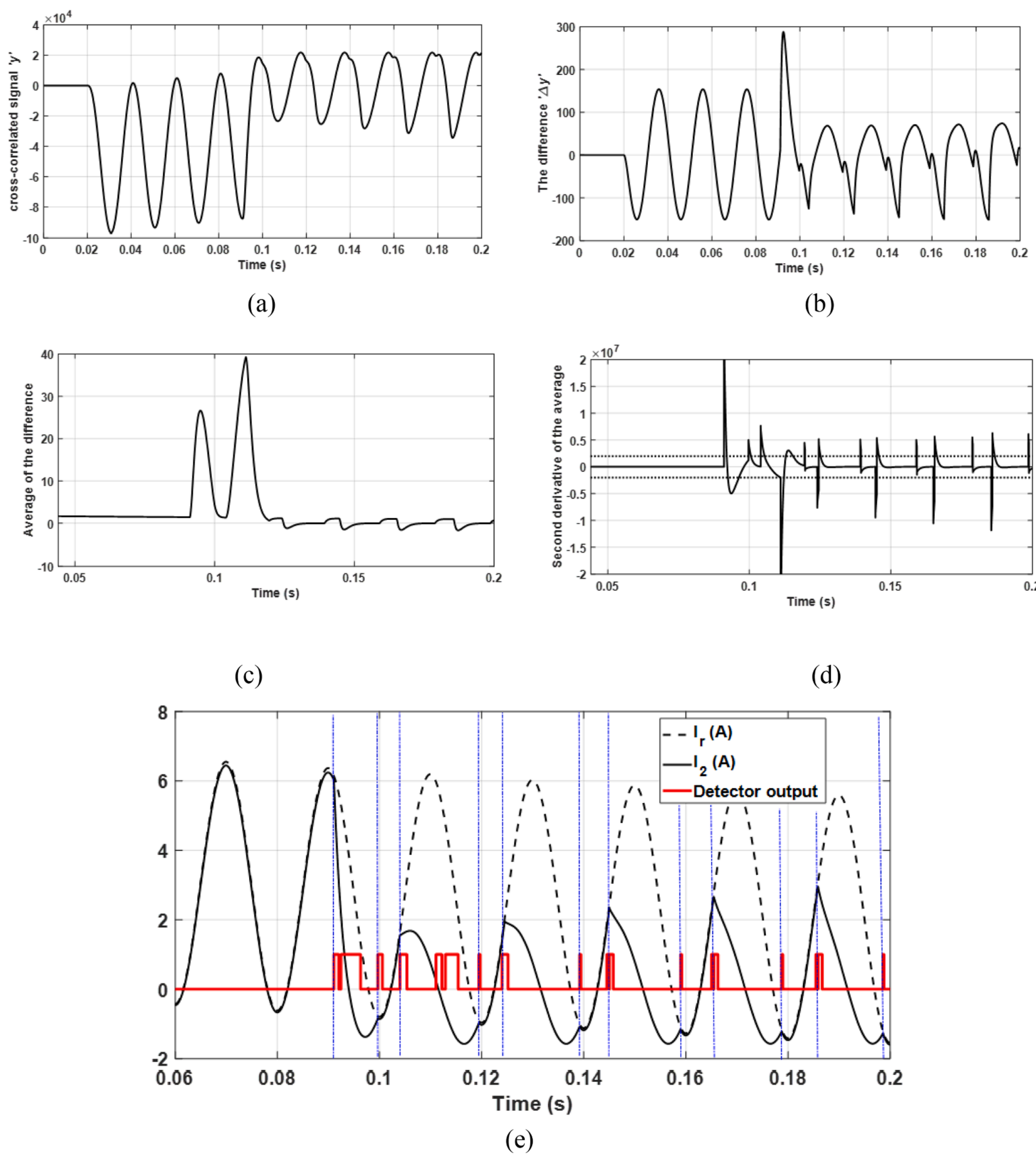

Fig. 6. Proposed method results; (a) the cross-correlated output signal after correlation; (b) the difference of the cross-correlated signal; (c) the average of the difference signal over one cycle; (d) the second derivate of the average compared to the preset threshold level; (e) the final proposed detector output along with the CT saturated secondary current.

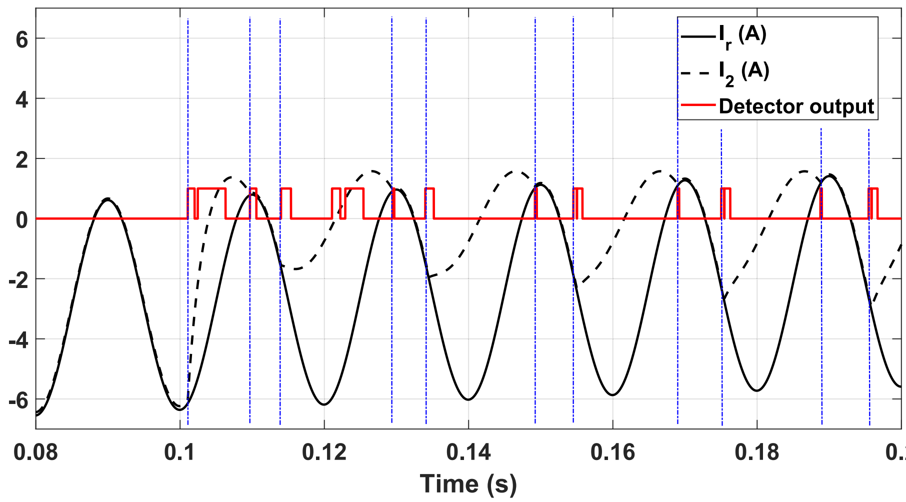

Fig. 7. The proposed detector output along with the CT saturated secondary current under different test conditions.

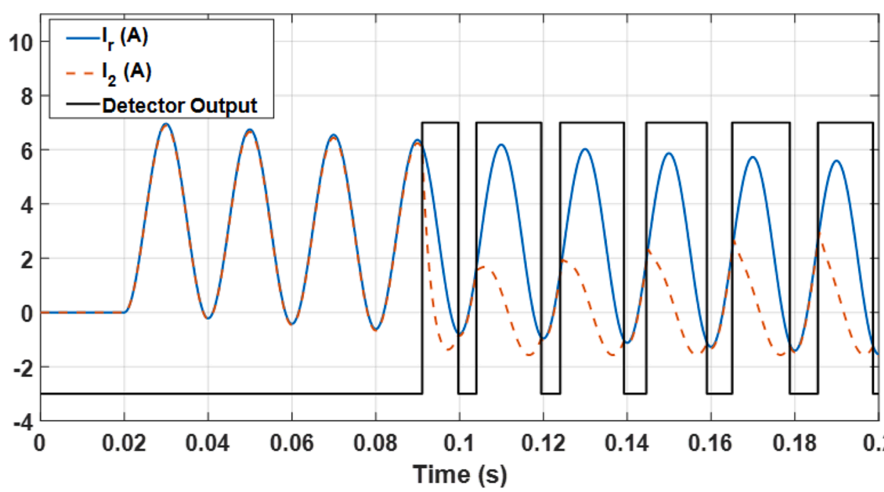

(a)

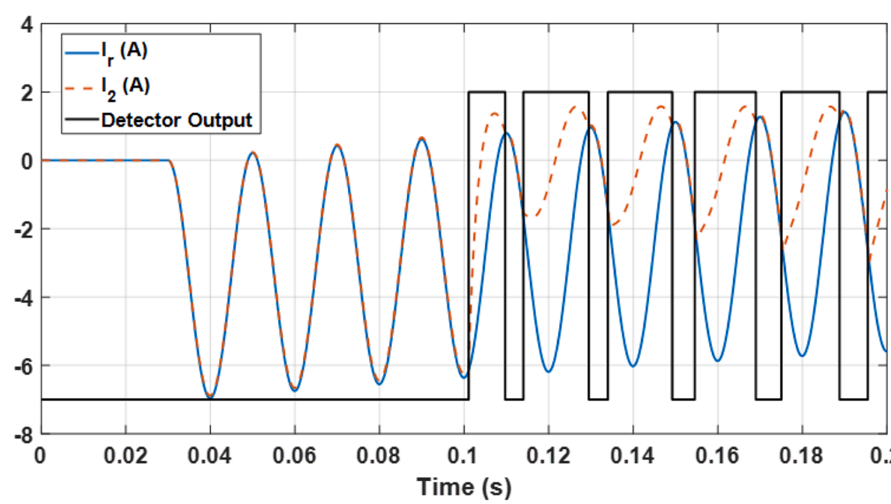

(b)

Fig. 8. The proposed detector output; (a) with closing the switch at 0.02 s; (b) with closing the switch at 0.03 s.

Additionally, the proposed method is validated under different test condition. The switch closure is delayed to 0.03 s, ensuring it does not coincide with the zero-crossing of the voltage. Under this scenario, the DC component in the secondary current becomes negative. Fig. 7 displays the CT secondary saturated current for this condition, along with the reference current and the output of the proposed detector. As shown, the results confirm that the output detector effectively identifies the moments when saturation begins and ends in each cycle.

7. Identifying saturation portions in secondary current

The proposed correlation-based method not only detects the start of CT saturation but also accurately identifies the boundaries of the saturated segment within each postfault cycle of the CT secondary current. This enhances the feasibility of rebuilding the CT secondary current for ensuring the proper operation of protection systems. Based on the results obtained from the test cases, the output detector generates indicative pulses at the key moments within the processed secondary current. It is evident that the rising edge of these pulses in the output detector precisely determines the start and end points of the saturated segment within the measured current. To further enhance reliability, the first post-fault cycle and half of the output detector are reanalysed to delineate the boundaries of the saturated segment more effectively. The successive pulses are combined if the falling edge of the first pulse is very close to the rising edge of the next one if they are separated by less than 10 % of one fundamental cycle. Further, the pulse is neglected if the rising edge of the detector is close to the zero-crossing of the measured current. These refining conditions are applied only during the first cycle and half after the first pulse in the detector output.

Considering the adopted test system, the final detector output for accurately identifying the boundaries of the saturated portion in the secondary current is presented in Fig. 8. Fig. 8a shows the output of the proposed saturation detection method for the test case where the circuit switch is closed at 0.02 s. As depicted, saturation starts at 0.091 s, and subsequent cycles reveal saturated regions within each cycle. The proposed method effectively detects these saturated portions throughout each cycle. In Fig. 8b, the results for a different test case are presented, where the switch is closed at 0.03 s. The results clearly highlight the method's ability to accurately identify the saturated regions in the processed secondary current. This accurate detection enables the reconstruction of the secondary current to replicate the primary current without the effects of saturation. Consequently, the primary reference current, free from saturation, can be reliably provided to protection relays, thereby preventing maloperation.

8. Rebuilding CT secondary current

With the proposed correlation-based algorithm, the unsaturated portions of the secondary current are effectively determined. With the above test cases, the unsaturated portion in each cycle of the secondary current is limited to approximately one-quarter of a cycle. Rebuilding the CT secondary current needs an algorithm that could extract the signal features based on the unsaturated portion. After identifying the unsaturated portion in the measured current, Kalman filter algorithm is utilized to extract the signal parameters and then rebuild the current [13,28]. The adopted Kalman filter technique for reconstructing the secondary current is provided as follows.

The processed measured current includes sinusoidal signal along with decaying DC component. The CT secondary current features are represented by state variables. If the CT secondary current is assumed to be:

$$i_2 = I\cos(\omega t + \varnothing) + i_{dc} \tag{6}$$

$$i_2 = I\cos(\omega t)cos(\varnothing) + I\sin(\omega t)\sin(\varnothing) + i_{dc} \tag{7}$$

where I is the amplitude of the assumed current signal, ω is the angular frequency, $\varnothing$ is the angle, and i_{dc} is the dc component accompanied in the assumed signal. The corresponding estimated state variables by Kalman filter are:

$$x_1 = Icos\varnothing,\ x_2 = Isin\varnothing,\ x_3 = i_{dc} \tag{8}$$

After estimating these variables, the CT secondary current is rebuilt as:

$$i_2 = x_1 cos(\omega t) + x_2 sin(\omega t) + i_{dc} \tag{9}$$

The proposed algorithm depends on executing Kalman filter on the unsaturated portion of the current signal to identify the state variables. Then, the CT current is rebuilt by the extracted features. The signal parameters are periodically extracted during each cycle within the unsaturated portion based on the obtained detector output.

After identifying the saturated portions in the measured current signal, the unsaturated parts are used to estimate the reference primary current. For the test case where the switch is closed at 0.02 s, the corresponding results are shown in Fig. 9. The unsaturated segments of the secondary current are highlighted in Fig. 9, where Kalman filtering is applied during these intervals. Fig. 9a displays the estimated state variables x_1 and x_2, which are utilized to reconstruct the sinusoidal component of the CT secondary current. These state variables are updated continuously during the unsaturated portions and retain their last calculated value during the saturated segments. In Fig. 9b, the estimated DC component is compared with the measured one. The DC current is estimated during the unsaturated parts of each cycle, and as shown, the estimated value closely aligns with the measured data. By extracting these features, the primary reference current is determined. Finally, Fig. 9c illustrates the reconstructed CT secondary current, which closely matches the reference current with the saturated portions successfully reconstructed.

The validation of the CT secondary current reconstruction using the proposed method is performed with another test case, where the switch is closed at 0.03 s. Fig. 10 presents the results for this test case. Fig. 10a and b show the state variables and DC component estimated through Kalman filtering in this scenario. The rebuilt secondary current is compared with the reference signal in Fig. 10c. As demonstrated, the proposed method effectively reconstructs the reference signal, enabling the accurate determination of the primary reference current to be provided to the protection system, thus addressing saturation-related issues.

9. Comparative study

The proposed method demonstrates superior robustness in detecting CT saturation compared to existing algorithms, particularly in the presence of noise. The most comparable algorithms in the literature rely on the second derivative of the measured secondary current and wavelet analysis of the signal [13–15]. In this comparative section the performance of each method is evaluated under noisy conditions to assess their robustness and effectiveness in detecting CT saturation. The tests were conducted by generating white noise using MATLAB tools and adding it to the measured CT secondary current, with a noise power level of 1 %.

Considering the second derivative method, Fig. 11a and b illustrate its performance, both without and with the influence of noise, respectively. As shown, the presence of noise significantly affects the results. In Fig. 11a, the second derivative method successfully identifies the moments of saturation with distinct spikes in the output—shorter spikes indicate the onset of saturation, while taller spikes mark the end of the saturated segments of the signal. However, in Fig. 11b, noise disrupts these results, making the shorter spikes less distinguishable and thereby hindering the clear identification of saturation points.

The wavelet analysis is assessed under the same noise level. Fig. 12a and b present the decomposition of the CT secondary current using the

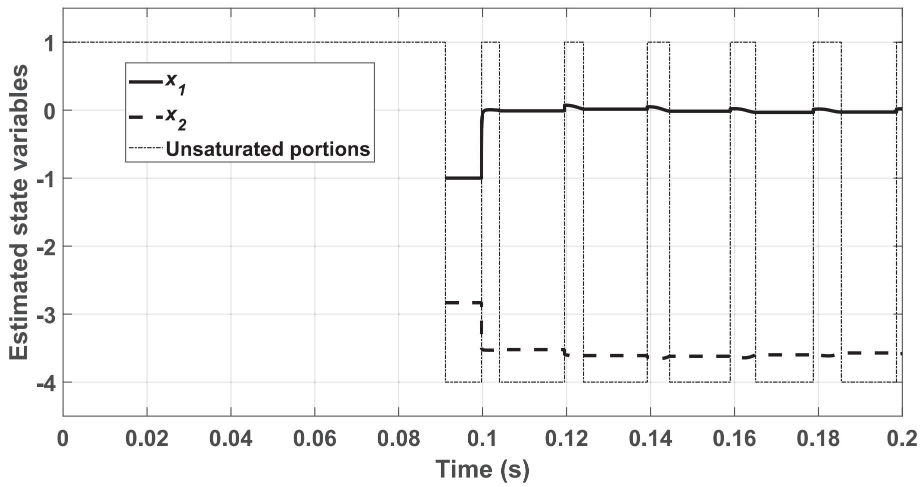

(a)

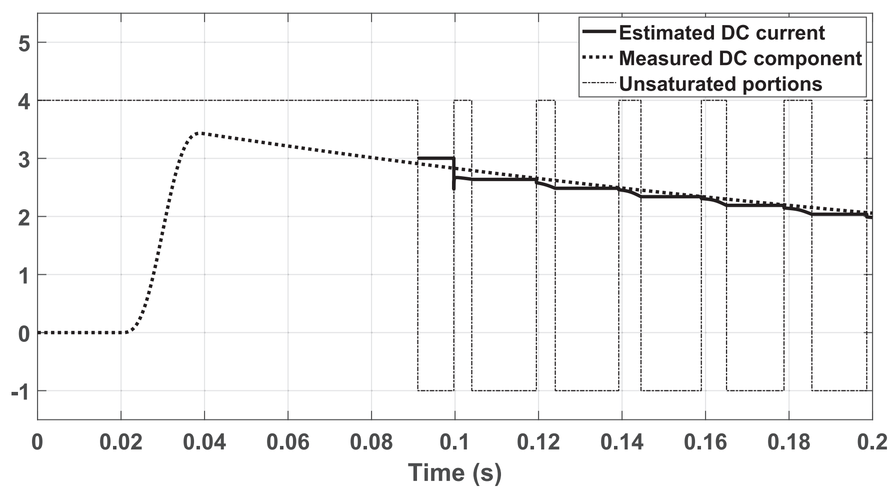

(b)

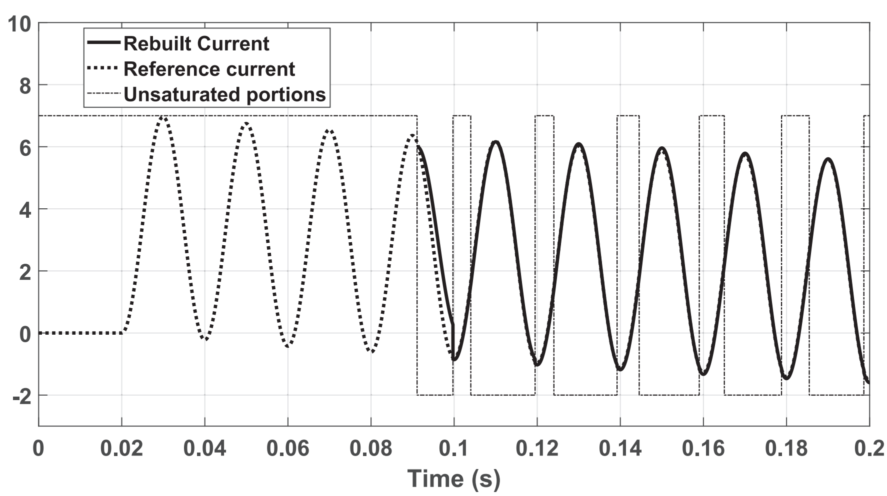

(c)

Fig. 9. Rebuilding the CT secondary current for the test case where the switch is closed at 0.02 s; (a) the estimated state variables by using Kalman filter during the unsaturated portions; (b) estimated dc component compared to the measured one; (c) The rebuilt and reference currents.

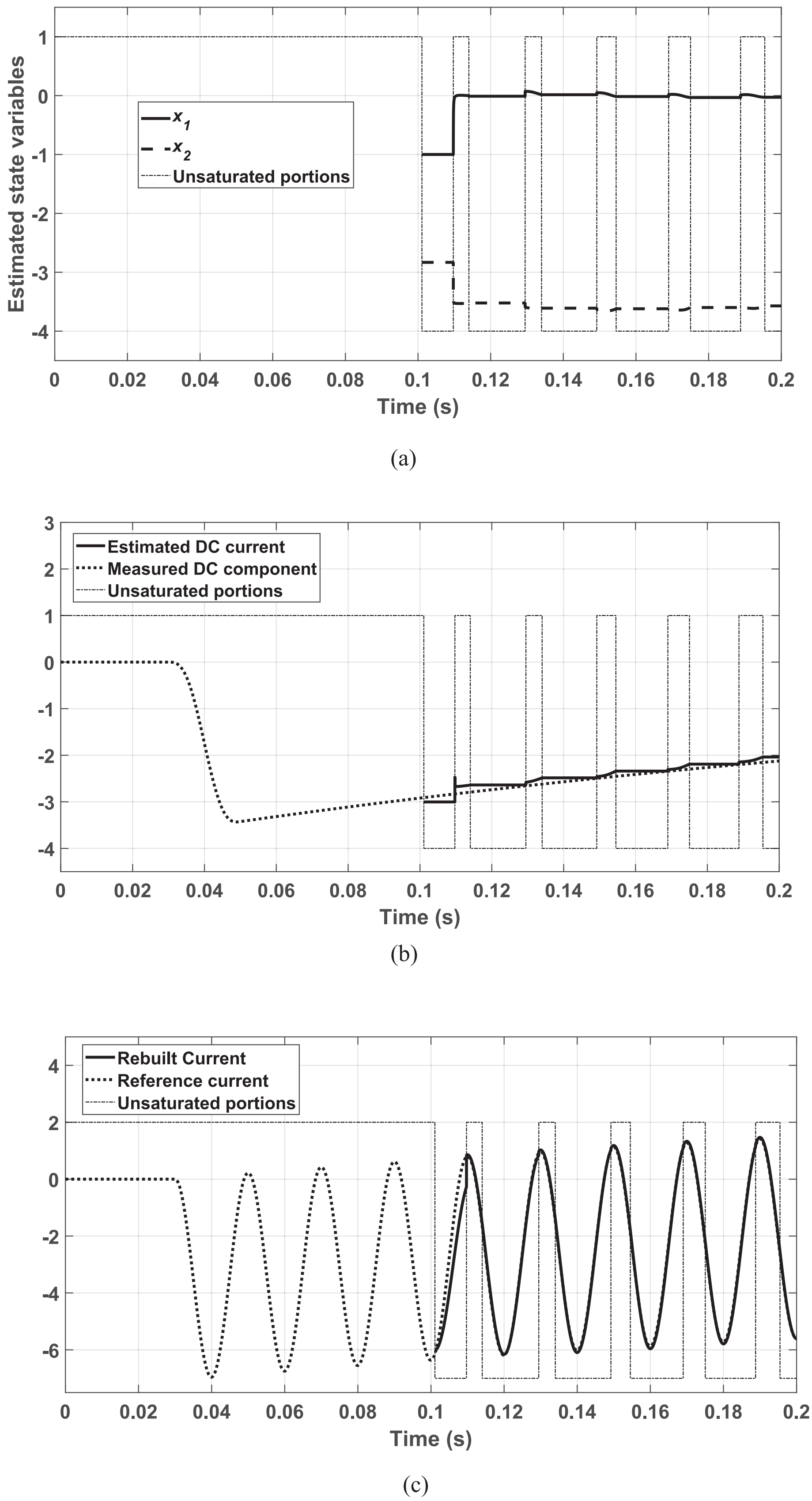

Fig. 10. Rebuilding the CT secondary current for the test case where the switch is closed at 0.03 s; (a) the estimated state variables by using Kalman filter during the unsaturated portions; (b) estimated dc component compared to the measured one; (c) The rebuilt and reference currents.

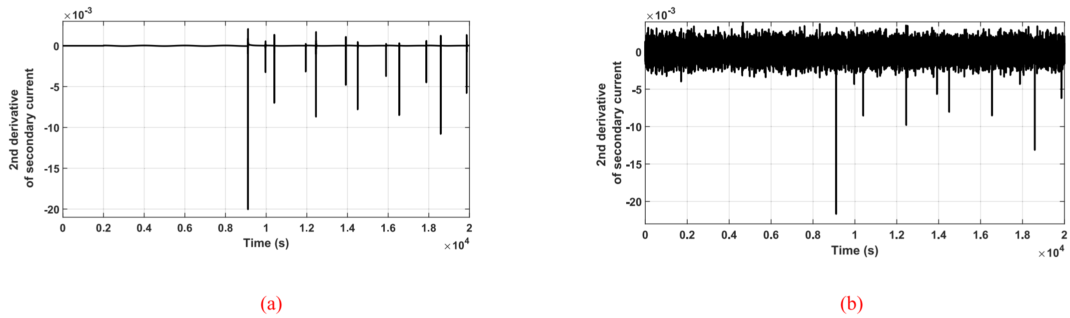

Fig. 11. The performance of the second derivative algorithm included in the method in [13] to detect CT saturation; (a) without noise; (b) with noise power level of 1%.

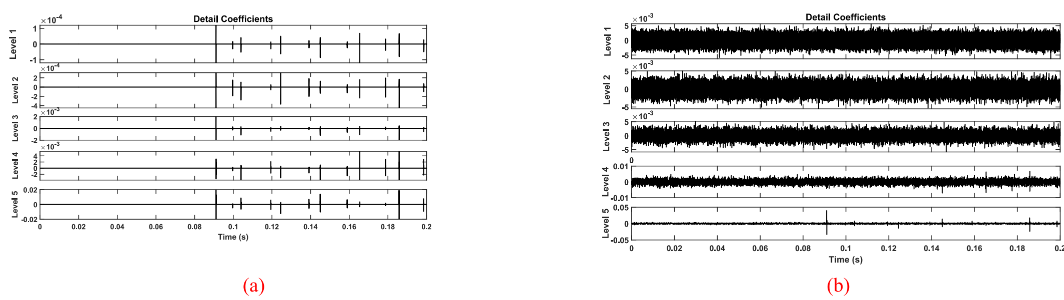

Fig. 12. The performance of the wavelet-based processing algorithm included in the methods in [14,15] to detect CT saturation; (a) without noise; (b) with noise power level of 1%.

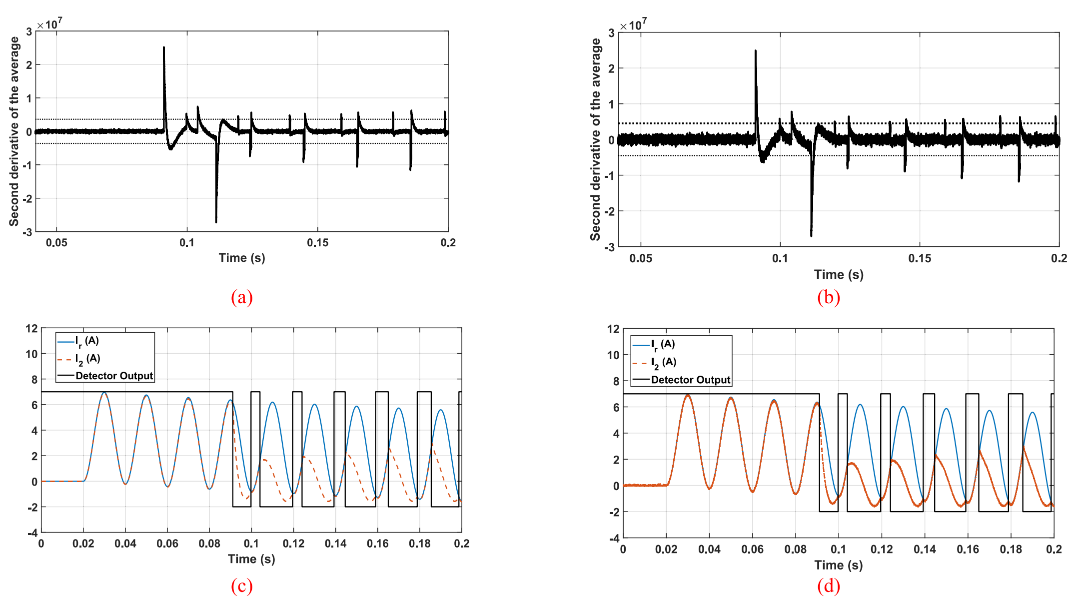

Fig. 13. The performance of the proposed method to detect CT saturation considering the same level of noise; (a) without noise; (b) with the same noise power level of 1%.

Discrete Wavelet Transform (DWT) with Daubechies wavelets (db4) across five levels. The resulting coefficients are plotted over time on a uniform time scale covering the entire duration of the CT secondary current signal. In Fig. 12a, the moments marking the beginning and end of the saturated portions are clearly identifiable. However, as shown in Fig. 12b, noise significantly degrades the results, rendering the coefficients unable to clearly indicate the saturation moments in the measured CT secondary current.

The proposed method is evaluated under the same noise level. Fig. 13 presents the results of this evaluation. Fig. 13a and b depict the operating variables utilized by the proposed method to detect CT saturation. As shown, the proposed method exhibits superior robustness, remaining unaffected by the noise level that adversely impacts existing methods in the literature. This robustness is evident in Fig. 13c and d, where the saturated portions are clearly identified despite the presence of noise.

However, the proposed method has a limitation in its sensitivity to higher noise levels, as its effectiveness decreases with increasing noise intensity. While it maintains robust performance under noisy conditions up to a noise power level of approximately 1.5 %, its accuracy progressively declines beyond this threshold.

10. Conclusions

A cross-correlation-based method is proposed for detecting saturation in current transformers. By processing the measured secondary current, the method accurately identifies the saturated portions. One of the key advantages of the proposed method is its independence from current transformer parameters, eliminating the need for additional hardware. Various test cases have been implemented, and the results demonstrate the method's accuracy and rapid response in detecting saturation. Furthermore, the reference primary current is effectively obtained using the Kalman filtering algorithm. The innovation of the proposed method lies in its use of the correlation concept, and it stands out for its robustness against noise. Unlike existing methods, which are significantly affected by noise, the proposed approach maintains strong performance up to noise power level 1.5 %. However, it does have a limitation: its effectiveness diminishes as noise levels increase, indicating sensitivity to higher noise intensities beyond this threshold.

CRediT authorship contribution statement

Mahmoud M. Elgamasy: Writing – original draft, Validation, Software, Methodology, Investigation, Formal analysis, Data curation, Conceptualization. **Mohamed S. Zaky:** Methodology, Formal analysis. **Ahmed F. Zobaa:** Writing – original draft, Methodology, Formal analysis. **Mahmoud A. Elsadd:** Writing – original draft, Validation, Software, Methodology, Investigation, Formal analysis, Data curation, Conceptualization.

Funding

The authors extend their appreciation to the Deanship of Scientific Research at Northern Border University, Arar, KSA for funding this research work through the project number "NBU-FPEJ-2025–1250-01.

Declaration of competing interest

The authors declare that they have no known competing financial interests or personal relationships that could have appeared to influence the work reported in this paper.

References

[1] Li S, Zhou J, Zhou F, Niu F, Deng W. A reduced current ripple overmodulation strategy for indirect matrix converter. IEEE Trans Ind Electron 2024. https://doi.org/10.1109/TIE.2024.3453934.
[2] Deng K, Yang L, Lu Y, Ma S. Multitype chatter detection via multichannelinternal and external signals in robotic milling. Measurement 2024;229. https://doi.org/10.1016/j.measurement.2024.114417.
[3] Li N, et al. Single-degree-of-freedom hybrid modulation strategy and light-load efficiency optimization for dual-active-bridge converter. IEEE J Emerg Select Top Power Electron 2024;12(4):3936–47. https://doi.org/10.1109/JESTPE.2024.3396340.
[4] Hajipour E, Vakilian M, Sanaye-Pasand M. Current-transformer saturation compensation for transformer differential relays. IEEE Trans Power Delivery 2015; 30(5):2293–302. https://doi.org/10.1109/TPWRD.2015.2411736.
[5] T. Smith and R. Hunt, Current transformer saturation effects on coordinating time interval, In: Conference Record of 2012 Annual IEEE Pulp and Paper Industry Technical Conference (PPIC), Portland, OR, USA, 2012, pp. 1-7, doi: 10.1109/PPIC.2012.6293016.
[6] Dashti H, Sanaye-Pasand M, Davarpanah M. Fast and reliable CT saturation detection using a combined method. IEEE Trans Power Delivery 2009;24(3): 1037–44. https://doi.org/10.1109/TPWRD.2009.2022666.
[7] Davarpanah M, Sanaye-Pasand M. Improved gapped-Core CT dimensioning algorithm considering relay and system requirements. IEEE Trans Power Delivery 2013;28(2):788–96. https://doi.org/10.1109/TPWRD.2012.2234485.
[8] Lesniewska E, Jalmuzny W. Influence of the number of core air gaps on transient state parameters of TPZ class protective current transformers. IET Sci Meas Technol 2009;3(2):105–12. https://doi.org/10.1049/iet-smt:20080005.
[9] Delzendeh M, Karegar HK. Current transformer saturation compensator by using negative voltage feedback. IEEE Trans Power Deliv 2019;35(3):1200–8. https://doi.org/10.1109/TPWRD.2019.2936449.
[10] Hajipour E, Vakilian M, Sanaye-Pasand M. Current-transformer saturation prevention using a controlled voltage-source compensator. IEEE Trans Power Deliv 2017;32(2):1039–48. https://doi.org/10.1109/TPWRD.2016.2580585.
[11] Jiao X, Zheng T. Remanent flux detection method for a protection current transformer based on fluxgate theory. Int J Electrical Power Energy Syst 2024;155. https://doi.org/10.1016/j.ijepes.2023.109591.
[12] Ji T, Shi M, Li M, Zhang L, Wu Q. Current Transformer saturation detection using morphological gradient and morphological decomposition and its hardware implementation. IEEE Trans Ind Electron 2017;64(6):4721–9. https://doi.org/10.1109/TIE.2017.2674578.
[13] Esmail EM, Elkalashy NI, Kawady TA, Taalab A-M-I, Lehtonen M. Detection of partial saturation and waveform compensation of current transformers. IEEE Trans Power Delivery 2015;30(3):1620–2. https://doi.org/10.1109/TPWRD.2014.2361032.
[14] Hong YY, Chang-Chian PC. Detection and correction of distorted current transformer current using wavelet transform and artificial intelligence. IET Gener Transm Distrib 2008;2(4):566–75. https://doi.org/10.1049/iet-gtd:20070383.
[15] Li F, Li Y, Aggarwal RK. Combined wavelet transform and regression technique for secondary current compensation of current transformers. IEE Proceed- Gen, Transmission Distribution, in Bath UK 2008:497–503. https://doi.org/10.1049/ip-gtd:20020296.
[16] Wang T, Han Q, Chu F, Feng Z. A new SKRgram based demodulation technique for planet bearing fault detection. J Sound Vib 2016;385:330–49. https://doi.org/10.1016/j.jsv.2016.08.026.
[17] Zeng W, Zhou P, Wu Y, Wu D, Xu M. Multi-cavitation states diagnosis of the vortex pump using a combined DT-CWT-VMD and BO-LW-KNN based on motor current signals. IEEE Sens J 2024. https://doi.org/10.1109/JSEN.2024.3446170.
[18] Erenturk K. ANFIS-based compensation algorithm for current-transformer saturation effects. IEEE Trans Power Delivery 2009;24(1):195–201. https://doi.org/10.1109/TPWRD.2008.2005882.
[19] Dang S, Xiao Y, Wang B, Zhang D, Zhang B, Hu S, et al. A high-precision error calibration technique for current transformers under the influence of DC bias. Energies 2023;16:7917. https://doi.org/10.3390/en16247917.
[20] Key S, Ko C-S, Song K-J, Nam S-R. Fast detection of current transformer saturation using stacked denoising autoencoders. Energies 2023;16:1528. https://doi.org/10.3390/en16031528.
[21] Moghimi Haji M, Vahidi B, Hosseinian SH. Current transformer saturation detection using gaussian mixture models. J Appl Res Technol 2013;11(1):79–87. https://doi.org/10.1016/S1665-6423.
[22] Rebizant W, Bejmert D. Current-transformer saturation detection with genetically optimized neural networks. IEEE Trans Power Deliv 2007;22(2):820–7. https://doi.org/10.1109/TPWRD.2007.893363.
[23] Yang S, Zhang Y, Hao Z, Lin Z, Zhang B. CT saturation detection and compensation: a hybrid physical model- and data-driven method. IEEE Trans Power Deliv 2022;37(5):3928–38. https://doi.org/10.1109/TPWRD.2022.3141550.
[24] Lin L, Liu J, Huang N, Li S, Zhang Y. Multiscale spatio-temporal feature fusion based non-intrusive appliance load monitoring for multiple industrial industries. Appl Soft Comput 2024;167. https://doi.org/10.1016/j.asoc.2024.112445.
[25] Fang H, Ma S, Wang J, Zhao L, Nie F, Ma X, Lü W, Yan S, Zheng L. Multimodal in-sensor computing implemented by easily-fabricated oxide-heterojunction optoelectronic synapses. Adv Funct Mater 2024;34(49):2409045. https://doi.org/10.1002/adfm.202409045.
[26] Zhou M, Zhao X, Luo F, Luo J, Pu H, Xiang T. Robust RGB-T tracking via adaptive modality weight correlation filters and cross-modality learning. ACM Trans Multimedia Comput, Commun Applic 2023;20(4):1–20. https://doi.org/10.1145/3630100.
[27] Liu K, Jiao S, Nie G, Ma H, Gao B, Sun C, Xin D, Saha TK, Wu G. On image transformation for partial discharge source identification in vehicle cable terminals of high-speed trains. High Voltage 2024;9(5):1090–100. https://doi.org/10.1049/hve2.12487.
[28] Girgis AA, Hart DG. Implementation of Kalman and adaptive Kalman filtering algorithms for digital distance protection on a vector signal processor. IEEE Trans Power Delivery 1989;4(1):141–56. https://doi.org/10.1109/61.19200.

Mahmoud M. Elgamasy is currently a lecturer at Electrical Engineering Department, Menoufia University, Egypt. He received the BSc and MSc degrees from Electrical Power and Machines Engineering Department, Faculty of Engineering, Menoufia University, Egypt, in 2011 and 2015 respectively. He obtained the PhD in 2021 from Menoufia University through a joint supervision programme between Menoufia University and Birmingham University, UK. He was postgraduate research visiting student at Birmingham University, UK for pursuing the PhD. His research interests include power systems protection, renewable energy resources, High Voltage Direct Current (HVDC) transmission systems.

Mohamed S. Zaky was born in Menoufia, Egypt in 1978. He received the B.Sc., M.Sc., and Ph.D. degrees in Electrical Engineering from Menoufia University, Shebin El-Kom, Egypt, in 2001, 2005, and 2008, respectively. He became an Instructor with Menoufia University in 2002 and an Assistant Lecturer in 2006. From 2008-2013, he became an assistant Professor with the Department of Electrical Engineering, Faculty of Engineering; Menoufia University. From 2013-2018, he became an assistant Professor with the Department of Electrical Engineering, Faculty of Engineering; Menoufia University. In July 2018, Dr. Zaky was promoted with scientific excellence to Professor in the field of "Automatic Control" with the Department of Electrical Engineering, Faculty of Engineering; Menoufia University. Now, Dr. Zaky is a professor with Department of Electrical Engineering, College of Engineering, Northern Border University, Arar, Saudi Arabia. His research interests include control of electrical machines; stability analysis of control systems; observers and estimators, applications of power electronics, DSP-based real-time control, and sensorless control of electrical.

Ahmed Faheem Zobaa received his BSc (Hons), MSc, and PhD degrees in Electrical Power & Machines from Cairo University, Egypt, in 1992, 1997, and 2002, respectively. He received his Postgraduate Certificate in Academic Practice from the University of Exeter, UK 2010, and his Doctoral of Science from Brunel University of London, UK 2017. He was an Instructor from 1992–1997, a Teaching Assistant from 1997–2002, and an Assistant Professor from 2002–2007 at Cairo University, Egypt. From 2007 to 2010, he was a Senior Lecturer in renewable energy at the University of Exeter, UK. From 2010 to 2019, he was a Senior Lecturer in power systems at Brunel University of London, UK. He is a Reader in electrical and power engineering and a Member of the Brunel Interdisciplinary Power Systems Research Centre at Brunel University of London, UK. His main areas of expertise include power quality, (marine) renewable energy, smart grids, energy efficiency, and lighting applications. Dr Zobaa is the Executive Editor-in-Chief of Smart Grids and Sustainable Energy Journal. He is also an Editorial Board member, Editor, Associate Editor, and Editorial Advisory Board member for many international journals. He is a registered Chartered Engineer, Chartered Energy Engineer, European Engineer, and International rofessional Engineer. He is also a registered member of the Engineering Council, UK; the Egypt Syndicate of Engineers; and the Egyptian Society of Engineers. He is a Principal Fellow of the Higher Education Academy, UK; Fellow of the Institution of Engineering and Technology, Energy Institute, UK; the Chartered Institution of Building Services Engineers, UK; the Institution of Mechanical Engineers, UK; the Royal Society of Arts, UK, and the African Academy of Sciences. He is also a senior member of the IEEE.

MAHMOUD A. ELSADD was born in Idku, Egypt, on October 1, 1985. He received the B.Sc., M.Sc., and Ph.D. degrees in Electrical Engineering from Menoufia University, Shebin El-Kom, Egypt, in 2007, 2012, and 2016, respectively. He held the position of teaching assistant in 2007, then a lecturer in 2012, and an assistant professor in 2016 at the Department of Electrical Engineering, Faculty of Engineering, Menoufia University, Shebin El-kom, Egypt. In 2021, he became an associate professor at the Department of Electrical Engineering, Faculty of Engineering, Menoufia University, Shebin El-kom, Egypt. He is now chairman of the Department of Electrical Engineering, Faculty of Engineering, Damanhour University, Egypt. His research interests include fault management in smart grids using various control schemes, security and privacy protection within smart grids, HVDC link protection, optimization techniques for power system operation, control system design, applications of artificial intelligence, power system protection, and renewable energy integration into power systems: challenges and solutions.